Soil Moisture Active and Passive (SMAP) White-Painted Expanded Polystyrene (EPS) Radome Survivability Test

Rebecca Mikhaylov[1], Eug Kwack[2], Matthew Stegman[3], Douglas Dawson[4], and Pamela Hoffman[5]
Jet Propulsion Laboratory, California Institute of Technology, Pasadena, California, 91109

NASA's SMAP Mission launched in January 2015 into a 685 km near-polar, sun-synchronous orbit. The SMAP instrument architecture incorporates an L-band radar and radiometer which share a common feedhorn and mesh reflector. The instrument rotates about the nadir axis at approximately 15 rpm, thereby providing a conically scanning wide swath antenna beam that is capable of achieving global coverage within three days. The radiometer and its associated electronics have tight thermal stability requirements in order to meet the required surface emittance measurement precision from space. Maintaining the thermal stabilities is quite challenging because the radiometer is located on a spinning platform that can either be in full sunlight or eclipse, and thus exposed to a highly transient environment. Stability requirements were met by integrating a light-weight Expanded Polystyrene (EPS) radome into the design to prevent solar illumination of the feed horn interior. The radome was painted white since the thermo-optical properties of bare sunlit EPS degrade rapidly over the three-year mission. Milling of the EPS and solvent within the white paint created cavities on the EPS surface which may introduce localized hot spots possibly violating the EPS glass transition temperature of 96 ºC and leading to structural integrity concerns. A three-day thermal test was conducted in a vacuum chamber to verify survivability of the radome during a simulated non-spin fault condition at end of mission. A portable solar simulator illuminated the test article and the beam irradiance was kept nearly constant during the entire 50 hour test, except during the first hour which simulated the expected 79 ºC on-orbit surface temperature of the radome. The test article survived based on the established pass criteria for three separate metrics: dimensional, optical property, and color. If any hot spots exist locally, they did not cause any observable permanent deformation when compared to pre- and post-test images. The test results increase confidence that there is a high probability that the radome will survive the worst-case scenario of a no-spin fault condition at the end of mission.

Nomenclature

α	=	solar absportivity
DSLR	=	Digital single-lens reflex
EPS	=	Expanded Polystyrene
GSFC	=	Goddard Space Flight Center
IR	=	Infrared
JPL	=	Jet Propulsion Laboratory
NASA	=	National Aeronautics and Space Administration
PC	=	Personal Computer
PDM	=	Product Delivery Manager
rpm	=	revolutions per minute
SMAP	=	Soil Moisture Active and Passive

[1] Instrument Thermal Engineer, Instrument Mechanical Thermal Subsystem, Mail Stop 125-123
[2] Lead Instrument Thermal Engineer, Instrument Mechanical Thermal Subsystem, Mail Stop 125-123
[3] Mechanical Cognizant Engineer, Instrument Mechanical Thermal Subsystem, Mail Stop 303-410
[4] Radiometer System Engineer, Instrument Systems Engineering, Mail Stop 168-314
[5] Mechanical Thermal Subsystem PDM, Instrument Mechanical Thermal Subsystem, Mail Stop 303-422

I. Introduction

The Soil Moisture Active Passive (SMAP) Mission, launched by the National Aeronautics and Space Administration (NASA) in 2015, will make global measurements of soil moisture and its freeze/thaw state by implementing an active radar and a passive radiometer that share a common L-band feedhorn and a conically scanning six-meter mesh reflector antenna (Figure 1). Direct observations of soil moisture and freeze/thaw state from space will allow significantly improved estimates of water, energy, and carbon transfers between the land and the atmosphere, which in turn will lead to enhanced weather and climate forecasts, and improved flood prediction and drought monitoring capability.

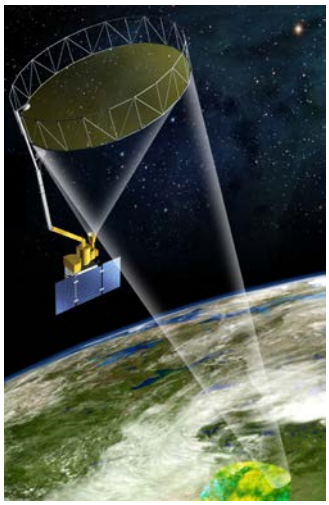

Figure 1. SMAP observatory with spinning 6m deployable mesh reflector antenna. The active radar and passive radiometer share a common L-band feedhorn with radome.

Development of the SMAP instrument suite is by a NASA partnership between the Jet Propulsion Laboratory (JPL) in Pasadena, California and the Goddard Space Flight Center (GSFC) in Greenbelt, Maryland. The SMAP mission formulation including the measurement approach, mission requirements, and data products were discussed, and the state-of-the-art associated with existing active/passive L-band microwave systems were summarized in previously published papers[1][2][3][4][5]. SMAP's unique nadir-spinning antenna platform generates a large swath that enables better than three day global coverage.

The rotating dual-frequency radiometer and radar share a common feedhorn which is closed by an Expanded Polystyrene (EPS) radome to prevent solar entrapment that adversely affects front end thermal stability[6]. A thermal coating of white paint (S13GP:6N/LO-1) was baselined due to the fast degradation of bare EPS optical properties. Mechanical cutting of the radome (instead of laser cutting) increased the surface roughness of the bare EPS. When the white paint was applied, the effective absorptivity of the painted radome increased from smooth-surface values. Using optical property measurements from the flight radome (α = 0.27) and degradation effects for a three-year mission ($\Delta\alpha$= 0.26), an effective absorptivity is expected to be 0.53 at the end of mission. A three-day thermal test was conducted in a three-foot diameter thermal vacuum chamber to verify survivability of the SMAP instrument radome during a simulated non-spin fault condition at end of mission.

II. Test Objective

Due to the EPS surface irregularities during paint application, wells and pinholes exist as part of the paint structure. Depending on the diameter and depth of these features and the varying thickness of white paint, it is possible that a localized spot could exceed the EPS glass transition temperature (the regime starts at 96 ºC). The concern is that the wells and pinholes may be exposed to a temperature greater than the start of the glass transition regime although the remaining paint structure is within qualification limits (< 86 ºC). The test objective was to subject the test article while in vacuum to a pre-determined solar flux value that produces the expected radome surface temperature for the end-of-mission, no-spin fault condition to verify the radome survivability and assess the solar-trapping effects on the radome surface with white paint that is pitted with cavities due to the milling of the EPS surface.

III. Test Article and Set-Up

The test article was two coupons from the flight radome paint process (Figure 2). Each coupon was 3.25"L x 3.25"W x 1" D. White paint was applied at the same time as the flight radome unit. The coupons had not been subjected to any additional thermal tests.

A portable solar simulator illuminated the test article through the quartz window of the vacuum chamber (Figure 3). The Spectrolab X-25 Solar Simulator beam is capable of producing up to 2.5 solar constants and includes a filter that produces a square illumination of approximately 9" x 9" at the 17.75" diameter Quartz window cover location. The beam irradiance was kept nearly constant (near 1725 W/m^2 at the center of beam) during the entire 50 hour test except during the first hour which simulated the expected 79 ºC on-orbit surface temperature of the radome.

The test article was mounted within a frame. The frame was then hung from the chamber rail using fixed length wire along with two calibration targets positioned at the same depth from the chamber door (Figure 4). The radome

Figure 2. EPS Test Article (two coupons)

was too fragile and too light weight to accommodate thermal sensors for direct temperature measurements. Instead, the calibration targets and beam were used to drive the two radome coupons to 76 ºC and 72 ºC respectively (delta due to solar flux and absorptivity variations of each coupon), and dimensional measurements pre- and post-test of the test article were used to investigate any changes in the radome due to localized hot spots.

IV. Instrumentation

Thermocouples were utilized to monitor temperature throughout the test. Additionally, a Nikon D2X DSLR camera running on a power supply captured time-lapse photographs at one frame per minute for documentation purposes using a laptop PC as the intervalometer (Figure 3). The images were used to examine any color and dimensional changes during the test and to produce a Quicktime movie which plays back in 100 seconds at the standard rate of 30 frames per second.

Figure 3. Side view of solar simulator and thermal vacuum chamber

Figure 4. Test Article set-up within thermal vacuum chamber

V. Test Results and Discussion

The temperature data for the calibration targets, shroud, window and door for the 50 hour test period are shown in Figure 5. The initial beam intensity was set near one maximum solar constant (1420 W/m^2) to ensure the test article temperature was near acceptable flight limits. Thirty minutes later, the test article was visually examined through the chamber window and no changes in color or structural integrity were observed. The beam intensity was then increased to 1585 W/m^2 (99 A) and held another 30 minutes. After another visual examination, finally, the beam intensity was increased to the target value of 1725 W/m^2 (103 A).

A test target temperature of 74 ºC was established based on the initial coupon absorptivity measurements of 0.21 and 0.23 and the predicted degradation of $\Delta\alpha = 0.26$. The temperature predictions in Figure 6 are based on the pre-test optical property measurements for five locations on each coupon and linear interpolation of beam intensity. At a target value of 1725 W/m^2 (103 A), the center of each test coupon is predicted to be 72 ºC and 76 ºC, respectively, which is close to the test target temperature of 74 ºC. The target temperature slowly decreased and around 23 hours, the current was increased from 103 A to 105 A resulting in an increase of 1 ºC in the test article temperatures. The test was terminated at 50 hours without any visible color or dimensional changes. Three different types of

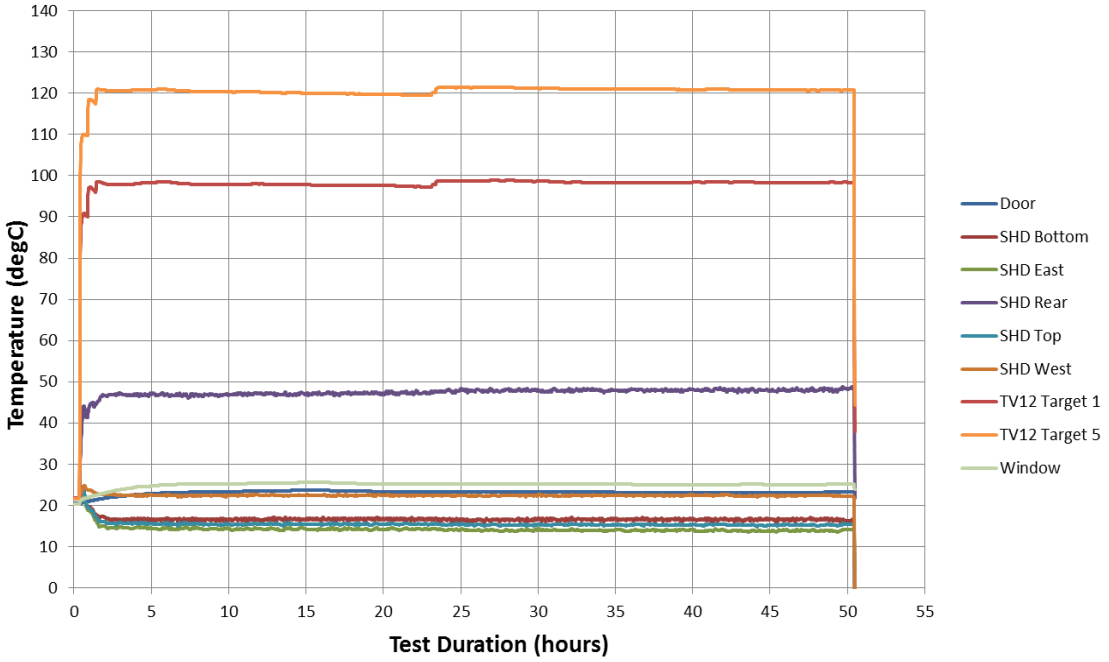

Figure 5. Survivability test temperature plot

measurements were made pre- and post-test on both test coupons to assess radome survivability: optical property meaurements, dimensional measurements, and color.

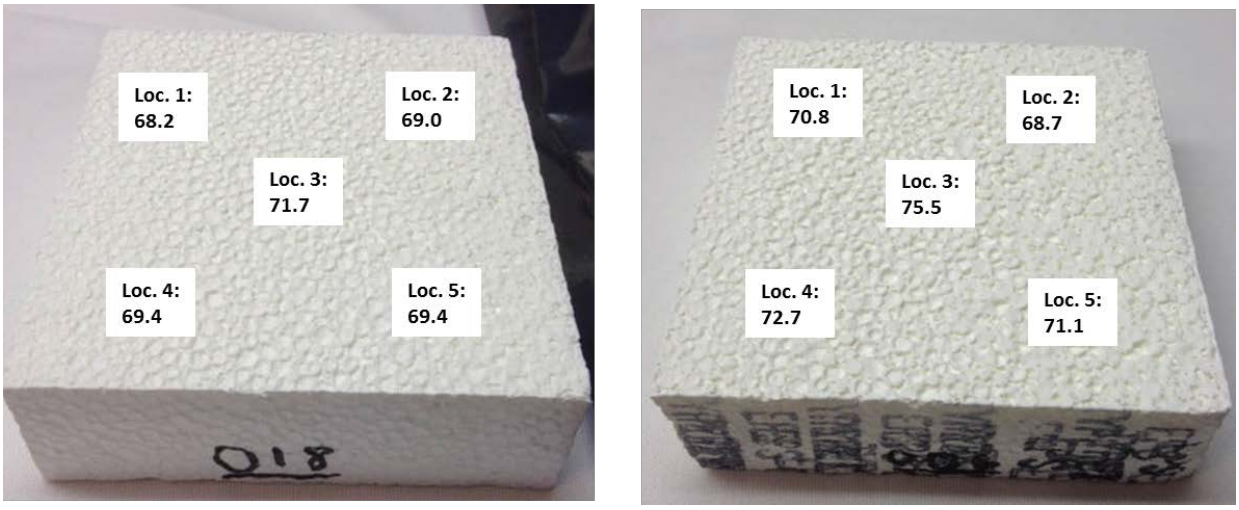

Figure 6. Survivability test temperature predictions and measurement locations

Table 1. Radome coupon optical property measurements

		Solar Absorptivity											IR Emissivity		
Sample	Location	pre	Avg	$(X_i - X_{avg})^2$	s	Median	post	Avg	$(X_i - X_{avg})^2$	s	Median	change, %	pre	post	change, %
006	1	0.208	0.218	0.0001082	0.010	0.220	0.197	0.214	0.000276	0.008	0.217	-5.3	0.902	0.908	0.67
	2	0.208		0.0001082			0.216		5.76E-06			3.8	0.905	0.899	-0.66
	3	0.233		0.0002132			0.22		4.1E-05			-5.6	0.904	0.912	0.89
	4	0.22		2.56E-06			0.218		1.94E-05			-0.9	0.907	0.91	0.33
	5	0.223		2.116E-05			0.217		1.16E-05			-2.7	0.909	0.904	-0.55
018	1	0.197	0.204	4.624E-05	0.008	0.201	0.196	0.200	0.000016	0.012	0.196	-0.5	0.899	0.901	0.22
	2	0.196		6.084E-05			0.222		0.000484			13.3	0.901	0.903	0.22
	3	0.207		1.024E-05			0.2		0			-3.4	0.895	0.906	1.23
	4	0.218		0.0002016			0.194		3.6E-05			-11.0	0.896	0.9	0.45
	5	0.201		7.84E-06			0.188		0.000144			-6.5	0.902	0.906	0.44

A. Optical Property Measurements

Pass/Fail criteria were established that the optical properties shall be within 20% of baseline measurements: 10% assumed for measurement error plus 10% for the actual property change. Measurement locations and corresponding pre- and post-test measurement values are documented in Figure 6 and Table 1. The variations in the solar absorptivity measurements are more than expected but still within the pass criteria. The variations in absorptivity measurements are attributed to measurement source error as well as the inability to repeat the exact measurement location with the source sensor (and size differences in the pinhole/well/cavity seen by the sensor at those two slightly different locations); an apparent 2% net decrease was observed. These assumptions are not a concern since the change in measurements largely trend downward. Additionally, there is a small increase in IR emissivity but also within the pass criteria.

B. Dimensional Measurements

The average EPS grain diameter is about 0.125". Pass/fail criteria was established that dimensions post-test shall be within 0.125" of the baseline measurements; 0.125" would be a visible change. Additionally, material shall be free of any holes across thickness of EPS sample (thickness defined between top painted surface and bottom surface).

C. Color

Real-time images were used to examine any color and dimensional changes during the test (Figure 7), and none were seen. Previous EPS testing indicated a yellow or brown discoloration due to extended exposure. The real-time images were initially examined regularly every hour for the first 12 hours and then randomly a few times a day until test completion. As part of post-production, a grid was overlaid the pre- and post-test images to better visualize and help quantify any potential changes. The coupons were examined post-test on a bench top with no visible changes or through-holes.

VI. Conclusion

The test article was exposed to a solar beam for a period of 50 hours resulting in surface temperatures near 76 ºC at the center of each coupon. Using the coupon optical property data, a maximum surface temperature of 74 ºC is expected during the end of mission fault condition with no-spin. The two EPS coupons survived the test based on the established pass criteria for three separate metrics: dimensional, optical property, and color. There were no visual changes in the dimensional or structural integrity of the two coupons. The test produced a 2% net decrease in the average solar absorptance of each coupon based on five measurements per coupon. The suspected cause for this is the location variation of the measurement source sensor in the pre- and post-test measurements. This deviation is well within the standard deviation of the measurement data set. If any hot spots exist locally, they did not cause any observable permanent deformation when comparing scaled coupon photographs before and after the test. No EPS color or dimensional changes were visible in the 100 second movie created from photos taken at 1 frame/minute during the entire test. The test results bolster confidence that there is a high probability the radome will survive under the worst-case scenario of a no-spin fault condition at the end of mission.

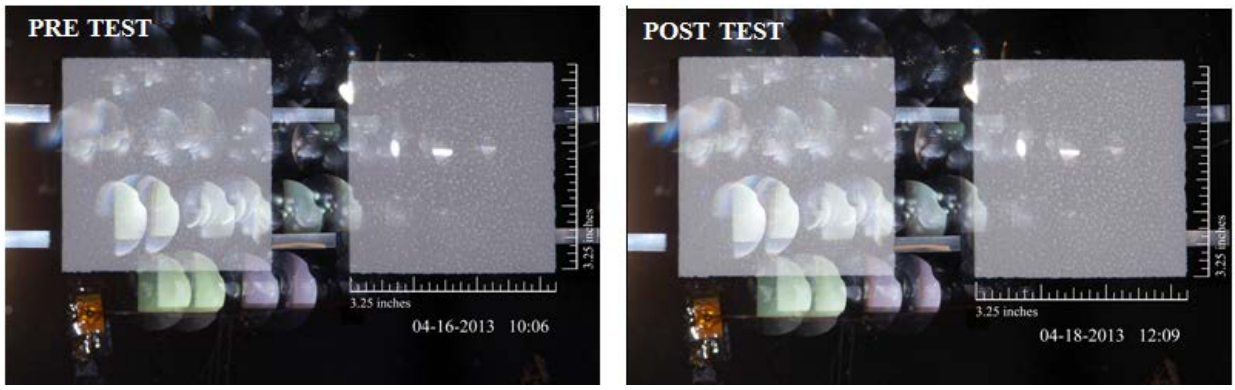

Figure 7. Pre- and Post-Test Radome Coupon Images with Scale to Evaluate any Dimensional Changes

Acknowledgments

The research was carried out at the Jet Propulsion Laboratory, California Institute of Technology, under a contract with the National Aeronautics and Space Administration. Additionally, the authors would like to acknowledge the following people for their contribution to the successful completion of this test:

- Eric Oakes for optical property measurement coordination
- Gus Forsberg for test definition
- Jose Rivera for definition of the pass/fail criteria
- Mihail Petkov for scanning electron microscope services
- Rich Frisbee for assembly of the test article and installation inside the chamber
- Sandro Torres for instrumentation
- Simeon Young, Mike Sachse, and Anton Ovcharenko for test support
- Stephanie Chan for thermal conductivity measurement coordination
- Thom Wynne for imaging services used during and post test.

References

[1] Entekhabi, D., Njoku, E.G., O'Neill, P.E., Kellogg, K., Crow, W., Edelstein, W., et. al., "The Soil Moisture Active Passive (SMAP) Mission," *Proceedings of the IEEE,* Vol. 98, No. 5, IEEE, Boston, MA, 2010, pp. 704-716.

[2] Entekhabi, D., Njoku, E., O'Neill, P., Spencer, M., Jackson, T., Entin, J., Im, E., and Kellogg, K., "The Soil Moisture Active/Passive Mission (SMAP)," *Geoscience and Remote Sensing Symposium, 2008. IGARSS 2008. IEEE International,* Vol. 3, IEEE, 2008, pp. III - 1-III - 4.

[3] Entekhabi, D., Jackson, T.J., Njoku, E., O'Neill, P., Entin, J., "Soil Moisture Active/Passive (SMAP) Mission Concept," *Atmospheric and Environmental Remote Sensing Data Processing and Utilization IV: Readiness for GEOSS II,* SPIE, Vol. 7085, 2008, pp. 70850H-1-70850H-6.

[4] Kim, S., van Zyl, J., McDonald, K., and Njoku, E., "Monitoring surface soil moisture and freeze-thaw state with the high-resolution radar of the Soil Moisture Active/Passive (SMAP) mission," *Radar Conference, 2010 IEEE,* 2010, pp. 735-739.

[5] O'Neill, P., Entekhabi, D., Njoku, E., and Kellogg, K., "The NASA Soil Moisture Active Passive (SMAP) Mission: Overview," *Geoscience and Remote Sensing Symposium (IGARSS), 2010 IEEE International,* IEEE, 2010, pp. 3236-3239.

[6] Stegman, M., "SMAP Antenna Feed Radome: Design, Development, and Test," *AERO, 2011, IEEE Aerospace Conference,* IEEE Aerospace Conference 2011, pp. 1-14, doi:10.1109/AERO.2011.5747502